Supporting Information

Potassium–Telluroether Interactions: Structural Characterisation and Computational Analysis

Novan A. G. Gray,[a] James F. Britten[b] and David J. H. Emslie*[a]

[a] Department of Chemistry & Chemical Biology, McMaster University, 1280 Main Street West, Hamilton, Ontario, L8S 4M1, Canada

[b] McMaster Analytical X-ray Diffraction Facility, McMaster University, Hamilton, Ontario, L8S 4M1, Canada

Table of Contents

General Details. An argon-filled MBraun UNIlab glove box equipped with a –30 °C freezer was employed for the manipulation and storage of all oxygen- and moisture- sensitive compounds. Air-sensitive reactions were performed on a double-manifold high-vacuum line equipped with an Edwards RV 12 vacuum pump using standard techniques. H[ASe_2^{Tripp2}], KCH_2Ph,[1] H[ATe_2^{Tripp2}], [K(ASe_2^{Tripp2})$(dme)_2$] (**1-Se**) and [K(ATe_2^{Tripp2})$(dme)_2$] (**1-Te**) were synthesized following previously reported procedure.[2] Benzene and pentane were purchased from Sigma Aldrich. Hexanes, toluene and THF were purchased from Caledon, *o*-difluorobenzene was purchased from Oakwood, and deuterated solvents were purchased from Cambridge Isotope Laboratories, Inc.

Hexanes, pentane, THF, and toluene were initially dried and distilled at atmospheric pressure from sodium/benzophenone (Hexanes and THF) and sodium (toluene). *o*-difluorobenzene and benzene were dried by stirring over 4 Å molecular sieves for 1 week, degassing, and distilling under reduced pressure. All solvents were stored over an appropriate drying agent (THF, toluene, benzene, THF-d_8, C_6D_6 = Na/Ph_2CO; hexanes, pentane = Na/Ph_2CO/tetraglyme) and introduced to reactions or air-free solvent storage flasks via vacuum transfer with condensation at –78 °C or inside of an argon-filled glovebox. Argon gas was purchased from Air Liquide.

^1H, $^{13}C\{^1H\}$, $^{77}Se\{^1H]$, and $^{125}Te\{^1H\}$ NMR spectra of all air-sensitive samples were acquired at room temperature in J-Young tubes on either a Bruker AV-600 or AV-500 MHz spectrometer. ^1H and $^{13}C\{^1H\}$ spectra were referenced relative to the residual protio signals of the solvent (C_6D_6) or the solvent carbon resonances, respectively (C_6D_6: ^1H = 7.16 ppm; ^{13}C = 128.06 ppm). $^{77}Se\{^1H\}$, and $^{125}Te\{^1H\}$ spectra were referenced by indirect referencing from a ^1H NMR spectrum.[3] Peak assignments in the spectra of all new compounds were made with the aid of DEPT-q, COSY, HSQC, and HMBC experiments. All $^{13}C\{^1H\}$ signals are singlets unless otherwise specified.

X-ray crystallographic analyses were performed with suitable crystals coated in paratone oil on a Bruker Dual Source D8 Venture diffractometer using the IμS 3.0 Mo source at 70 W with a HELIOS Mo focusing optic (ELM33) in the McMaster Analytical X-ray (MAX) Diffraction Facility. Raw data was processed using XPREP (as part of the APEX v4 software) and solved by intrinsic (SHELXT)[4] methods. Structure refinement was performed with

SHELXL[5] in OLEX2.[6] Images were rendered using Ortep3 and POV-Ray. Combustion elemental analyses were carried out at McMaster University.

DFT Details. Geometry optimization calculations were conducted with ADF within the AMS DFT package (SCM, version 2022.103 or 2023.102).[7] Calculations were performed in the gas phase within the generalized gradient approximation using the 1996 Perdew−Burke−Ernzerhof exchange and correlation functional (PBE),[8] using the scalar zeroth-order regular approximation (ZORA)[9-13] for relativistic effects, and Grimme's DFT-D3-BJ dispersion correction.[14,15] These calculations were conducted using all-electron triple-ζ basis sets with two polarization functions (TZ2P), and fine integration grids (Becke[16,17] very good quality) with default convergence criteria for energy and gradients. Analytical frequency calculations[18-20] were performed to ensure that each geometry optimization led to an energy minimum. Quantum theory of atoms in molecules (QTAIM)[21] properties were obtained using the QTAIM keyword[7] with an analysis level of Full,[22-29] and NBO[30] analysis was carried out using NBO 6.0 within the AMS DFT package. DFT, NBO and QTAIM data for **1-Te*** has been published elsewhere.[2]

Potassium 4,5-bis(2,4,6-triisopropylphenyltellurido)-2,7,9,9-tetramethylacridanide · 2 THF [K(ATe_2^{Tripp2})$(THF)_2$] (**3-Te**)

Method A: H[ATe_2^{Tripp2}] (42.5 mg, 0.0474 mmol) and KCH_2Ph (7.4 mg, 0.057 mmol) was dissolved in ~2 ml of THF in a pre-weighed 25 ml round-bottom flask and stirred under argon for 15 minutes, the solution was then evaporated to dryness *in vacuo* and dried for 10 minutes leaving an orange residue. 50.8 mg (0.0471 mmol) of [K(ATe_2^{Tripp2})$(THF)_2$] (**3-Te**) was obtained in nearly quantitative yield (99 %).

Method B: [K(ATe_2^{Tripp2})$(dme)_2$] (**1-Te**) (42.9 mg, 0.0385 mmol) was dissolved in ~4 ml of THF and then subsequently dried *in vacuo* to yield an orange residue. The material was redissolved in ~4 ml of THF and evaporated to dryness, and then once more for a total of three cycles of dissolutions and evaporations. The residue was dried for 10 minutes then brought into a glovebox and collected. 30.5 mg (0.0283 mmol) of [K(ATe_2^{Tripp2})$(THF)_2$] (**3-Te**) was obtained as a yellow solid in 73 % yield. **^{1}H NMR (C_6D_6, 600 MHz):** δ 7.34 (s, 4H, ArC*H*), 7.04 (s, 2H, AcridanC*H*), 6.67 (s, 2H, AcridanC*H*), 4.18-4.12 (sept, $J_{H\text{-}H}$ 6.83 Hz, 4H, *o*-C*H*Me_2), 3.56-3.54 (m, 8H, OCH_2), 2.93-2.87 (sept, $J_{H\text{-}H}$ 6.95 Hz, 2H, *p*-C*H*Me_2), 2.07 (s, 6H, C*Me*), 1.70 (s, 6H, CMe_2), 1.42-1.40

(m, 8H, CH_2), 1.38-1.37 (d, $J_{H\text{-}H}$ 6.88 Hz, 24H, *p*-CHMe_2), 1.29-1.28 (d, $J_{H\text{-}H}$ 6.98 Hz, 12H, *o*-CHMe_2). **^{13}C{^{1}H} NMR (C_6D_6, 150 MHz):** δ 156.14 (*o*-Aryl*C*), 150.29 (*p*-Aryl*C*), 147.15 (Acridan*C*Me), 129.86 (Acridan*C*H), ~128 (Acridan*C*), 125.58 (Acridan*C*H), 125.36 (Acridan*C*Te), 122.50 (Aryl*C*Te), 121.59 (Aryl*C*H), 112.04 (Acridan*C*N), 67.83 (O*C*H_2), 40.05 (*o*-*C*HMe$_2$), 37.06 (*C*Me$_2$), 35.68 (CMe_2), 34.68 (*p*-*C*HMe$_2$), 25.81 (*C*H_2), 25.41 (*o*-CHMe_2), 24.30 (*p*-CHMe_2), 21.06 (C*Me*). **^{125}Te{^{1}H} NMR (C_6D_6, 189 MHz):** δ 231.57 (s). **Anal. Calcd. for Method B.** $C_{55}H_{78}NTe_2O_2K$: C, 61.19; H, 7.28; N, 1.30%. **Found:** C, 61.20; H, 7.39; N 1.37%.

Potassium 4,5-bis(2,4,6-triisopropylphenyltellurido)-2,7,9,9-tetramethylacridanide · THF [K(ATe$_2^{Tripp2}$)(THF)] (**4-Te**)

[K(ATe$_2^{Tripp2}$)(THF)$_2$] (**3-Te**) (50.8 mg, 0.0471 mmol) was charged to a 25 ml round bottom flask and dried *in vacuo* for 60 minutes. The solid was collected in the glovebox and 24.1 mg (0.0239 mmol) of a yellow [K(ATe$_2^{Tripp2}$)(THF)] (**4-Te**) was obtained in 51% yield. **^{1}H NMR (C_6D_6, 600 MHz):** δ 7.34 (s, 4H, Ar*CH*), 7.04 (s, 2H, Acridan*CH*), 6.67 (s, 2H, Acridan*CH*), 4.18-4.12 (sept, $J_{H\text{-}H}$ 6.83 Hz, 4H, *o*-C*H*Me$_2$), 3.55-3.53 (m, 4H, OCH_2), 2.92-2.86 (sept, $J_{H\text{-}H}$ 6.95 Hz, 2H, *p*-C*H*Me$_2$), 2.07 (s, 6H, C*Me*), 1.70 (s, 6H, CMe_2), 1.42-1.40 (m, 4H, CH_2), 1.38-1.37 (d, $J_{H\text{-}H}$ 6.88 Hz, 24H, *p*-CHMe_2), 1.29-1.28 (d, $J_{H\text{-}H}$ 6.98 Hz, 12H, *o*-CHMe_2). **^{13}C{^{1}H} NMR (C_6D_6, 150 MHz):** δ 156.14 (*o*-Aryl*C*), 150.30 (*p*-Aryl*C*), 147.14 (Acridan*C*Me), 129.87 (Acridan*C*H), ~128 (Acridan*C*), 125.59 (Acridan*C*H), 125.38 (Acridan*C*Te), 122.49 (Aryl*C*Te), 121.60 (Aryl*C*H), 112.04 (Acridan*C*N), 67.83 (O*C*H_2), 40.05 (*o*-*C*HMe$_2$), 37.06 (*C*Me$_2$), 35.71 (CMe_2), 34.68 (*p*-*C*HMe$_2$), 25.80 (*C*H_2), 25.41 (*o*-CHMe_2), 24.30 (*p*-CHMe_2), 21.06 (C*Me*). **^{125}Te{^{1}H} NMR (C_6D_6, 189 MHz):** δ 231.57 (s). **Anal. Calcd.** $C_{51}H_{70}NTe_2OK$: C, 60.80; H, 7.00; N, 1.39%. **Found:** C, 60.28; H, 6.51; N 1.46%.

Potassium 4,5-bis(2,4,6-triisopropylphenyltellurido)-2,7,9,9-tetramethylacridanide [K(ATe$_2^{Tripp2}$)]$_x$ (**5-Te**)

[K(ATe$_2^{Tripp2}$)(THF)] (**4-Te**) (19.0 mg, 0.0189 mmol) was dissolved in ~1 ml of benzene and then evaporated *in vacuo* to yield an orange residue. The material was then redissolved in ~1 ml of benzene and once again evaporated to dryness. The solid was dried for 2 hours then brought

into a glovebox and collected. 12.4 mg (0.0133 mmol) of $[K(ATe_2^{Tripp2})]_x$ (**5-Te**) was collected as an orange solid in 70 % yield. X-ray quality crystals of **5-Te** were grown from *o*-difluorobenzene/pentane solution of **4-Te** cooled to –30 °C over 1 month. **^{1}H NMR (C_6D_6, 600 MHz):** δ 7.34 (s, 4H, ArC*H*), 7.04 (s, 2H, AcridanC*H*), 6.67 (s, 2H, AcridanC*H*), 4.18-4.12 (sept, $J_{H\text{-}H}$ 6.89 Hz, 4H, *o*-C*H*Me$_2$), 2.93-2.86 (sept, $J_{H\text{-}H}$ 6.92 Hz, 2H, *p*-C*H*Me$_2$), 2.07 (s, 6H, C*Me*), 1.70 (s, 6H, C*Me$_2$*), 1.38-1.37 (d, $J_{H\text{-}H}$ 6.20 Hz, 24H, *p*-CH*Me$_2$*), 1.29-1.28 (d, $J_{H\text{-}H}$ 6.93 Hz, 12H, *o*-CH*Me$_2$*). **^{13}C{^{1}H} NMR (C_6D_6, 150 MHz):** δ 156.15 (*o*-Aryl*C*), 150.30 (*p*-Aryl*C*), 147.14 (Acridan*C*Me), 129.89 (Acridan*C*H), ~128 (Acridan*C*), 125.61 (Acridan*C*H), 125.42 (Acridan*C*Te), 122.48 (Aryl*C*Te), 121.60 (Aryl*C*H), 112.02 (Acridan*C*N), 40.06 (*o*-*C*HMe$_2$), 37.06 (*C*Me$_2$), 35.68 (C*Me$_2$*), 34.68 (*p*-*C*HMe$_2$), 25.42 (*o*-CH*Me$_2$*), 24.30 (*p*-CH*Me$_2$*), 21.06 (C*Me*). **^{125}Te{^{1}H} NMR (C_6D_6, 189 MHz):** δ 231.17 (s). **Anal. Calcd.** $C_{47}H_{62}NTe_2K$: C, 60.36; H, 6.68; N, 1.50%. **Found:** C, 60.74; H, 6.70; N 1.54%.

Potassium 4,5-bis(2,4,6-triisopropylphenylselenido)-2,7,9,9-tetramethylacridanide · 2 THF $[K(ASe_2^{Tripp2})(THF)_2]$ (**3-Se**)

H$[ASe_2^{Tripp2}]$ (28.6 mg, 0.0358 mmol) and KCH_2Ph (5.1 mg, 0.039 mmol) was dissolved in ~3 ml THF and stirred under argon for 15 minutes, the solution was then evaporated to dryness *in vacuo* and dried for 10 minutes leaving a yellow residue. The solid was collected in the glovebox and 12 mg (0.012 mmol) of a compound of $[K(ASe_2^{Tripp2})(THF)_2]$ (**3-Se**) was obtained in 34% yield. X-ray quality crystals of **3-Se** (intergrown with **2-Se·hexane**) and **2-Se** (intergrown with **3-Se**) were grown from THF/hexanes solution of **1-Se** cooled to –30 °C over 2 days. **^{1}H NMR (C_6D_6, 600 MHz):** δ 7.32 (s, 4H, ArC*H*), 7.08 (s, 2H, AcridanC*H*), 6.42 (s, 2H, AcridanC*H*), 3.98-3.93 (sept, $J_{H\text{-}H}$ 6.87 Hz, 4H, *o*-C*H*Me$_2$), 3.54-3.52 (m, 8H, OC*H$_2$*), 2.90-2.83 (sept, $J_{H\text{-}H}$ 6.95 Hz, 2H, *p*-C*H*Me$_2$), 2.11 (s, 6H, C*Me*), 1.76 (s, 6H, C*Me$_2$*), 1.41-1.39 (m, 8H, C*H*$_2$), 1.30-1.29 (d, $J_{H\text{-}H}$ 6.71 Hz, 24H, *o*-CH*Me$_2$*), 1.27-1.26 (d, $J_{H\text{-}H}$ 6.88 Hz, 12H, *p*-CH*Me$_2$*). **^{13}C{^{1}H} NMR (C_6D_6, 150 MHz):** δ 154.27 (*o*-Aryl*C*), 150.20 (*p*-Aryl*C*), 146.12 (Acridan*C*Se), ~128 (Acridan*C*), ~128 (Aryl*C*Se), ~128 (Acridan*C*), 124.87 (Acridan*C*H), 124.40 (Acridan*C*H), 123.34 (Acridan*C*Me), 122.23 (Acridan*C*N), 122.23 (Aryl*C*H), 67.83 (O*C*H$_2$), 37.35 (*C*Me$_2$), 34.73 (*p*-*C*HMe$_2$), 34.71 (*o*-*C*HMe$_2$), 34.18 (C*Me$_2$*), 25.78 (*C*H$_2$), 24.92 (*o*-CH*Me$_2$*), 24.23 (*p*-CH*Me$_2$*), 21.32 (C*Me*). **^{77}Se{^{1}H} NMR (C_6D_6, 114 MHz):** δ 202.40 (s). **Anal. Calcd.** $C_{55}H_{78}NSe_2O_2K$: C, 67.25; H, 8.00; N, 1.43%. **Found:** C, 67.90; H, 7.86; N 1.81%.

Potassium 4,5-bis(2,4,6-triisopropylphenylselenido)-2,7,9,9-tetramethylacridanide · THF

[K(ASe_2^{Tripp2})(THF)] (**4-Se**)

[K(ASe_2^{Tripp2})$(THF)_2$] (**3-Se**) (6 mg, 0.061 mmol) was dried *in vacuo* in a pre-weighed flask on a vacuum line for 1 hour. The flask was brought back into the glovebox and 5.6 mg (0.061 mmol) of [K(ASe_2^{Tripp2})(THF)] (**4-Se**) was obtained in quantitative yield. **^{1}H NMR (C_6D_6, 600 MHz):** δ 7.32 (s, 4H, ArC*H*), 7.08 (s, 2H, AcridanC*H*), 6.43 (s, 2H, AcridanC*H*), 3.96-3.91 (sept, $J_{H\text{-}H}$ 7.00 Hz, 4H, *o*-C*H*Me_2), 3.57-3.55 (m, 4H, OCH_2), 2.90-2.83 (sept, $J_{H\text{-}H}$ 7.12 Hz, 2H, *p*-C*H*Me_2), 2.11 (s, 6H, C*Me*), 1.77 (s, 6H, CMe_2), 1.42-1.40 (m, 4H, CH_2), 1.30-1.29 (d, $J_{H\text{-}H}$ 6.71 Hz, 24H, *o*-CHMe_2), 1.27-1.26 (d, $J_{H\text{-}H}$ 6.88 Hz, 12H, *p*-CHMe_2). **^{13}C{^{1}H} NMR (C_6D_6, 150 MHz):** δ 154.24 (*o*-Aryl*C*), 150.22 (*p*-Aryl*C*), 146.13 (Acridan*C*Se), ~128 (Acridan*C*), ~128 (Aryl*C*Se), 124.89 (Acridan*C*H), 124.42 (Acridan*C*H), 123.37 (Acridan*C*Me), 122.24 (Acridan*C*N), 122.24 (Aryl*C*H), 67.83 (OCH_2), 37.35 (*C*Me_2), 34.73 (*p*-*C*HMe_2), 34.71 (*o*-*C*HMe_2), 34.61 (CMe_2), 25.80 (*C*H_2), 24.92 (*o*-CHMe_2), 24.23 (*p*-CHMe_2), 21.31 (C*Me*). **^{77}Se{^{1}H} NMR (C_6D_6, 114 MHz):** δ 202.13 (s). **Anal. Calcd.** $C_{51}H_{70}NSe_2OK$: C, 67.30; H, 7.75; N, 1.54%. **Found:** C, 67.72; H, 7.60; N 1.82%.

X-ray Crystal Structure of [K(ASe$_2$^{Tripp2})(THF)$_3$]·hexane (2-Se·hexane)

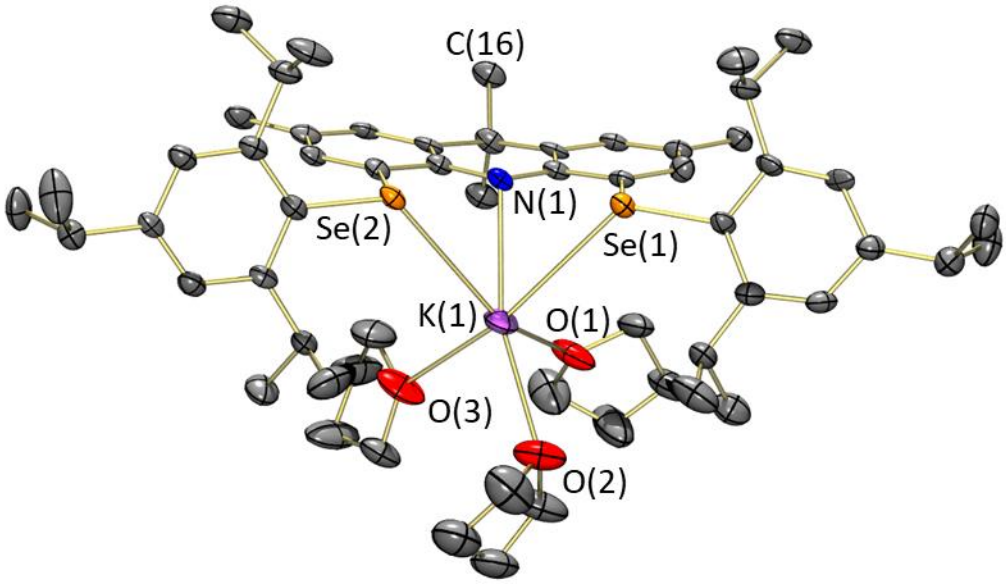

Figure S1. X-ray crystal structure of [K(ASe$_2$^{Tripp2})(THF)$_3$]·hexane (**2-Se**·hexane) (**2-Se**·hexane; with diffuse scattering along the *c*-axis suggesting intergrowth of **2-Se**·hexane {major} with **3-Se** {minor}). H atoms and hexane solvent molecule are omitted for clarity. Ellipsoids are drawn at 50% probability.

NMR Spectroscopy

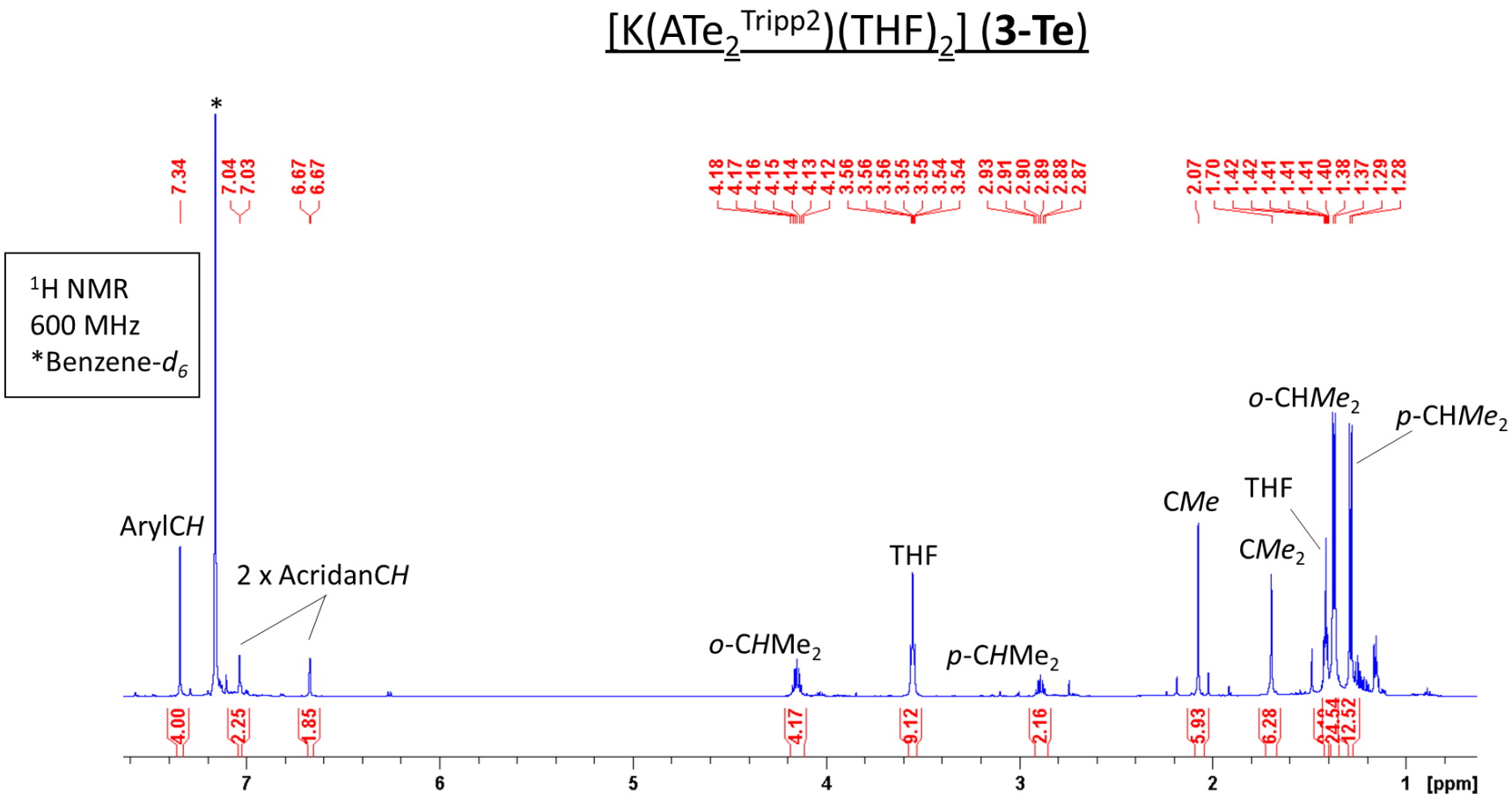

Figure S2. ^{1}H NMR spectrum of [K(ATe$_2^{Tripp2}$)(THF)$_2$] (**3-Te**) in C_6D_6 (298 K).

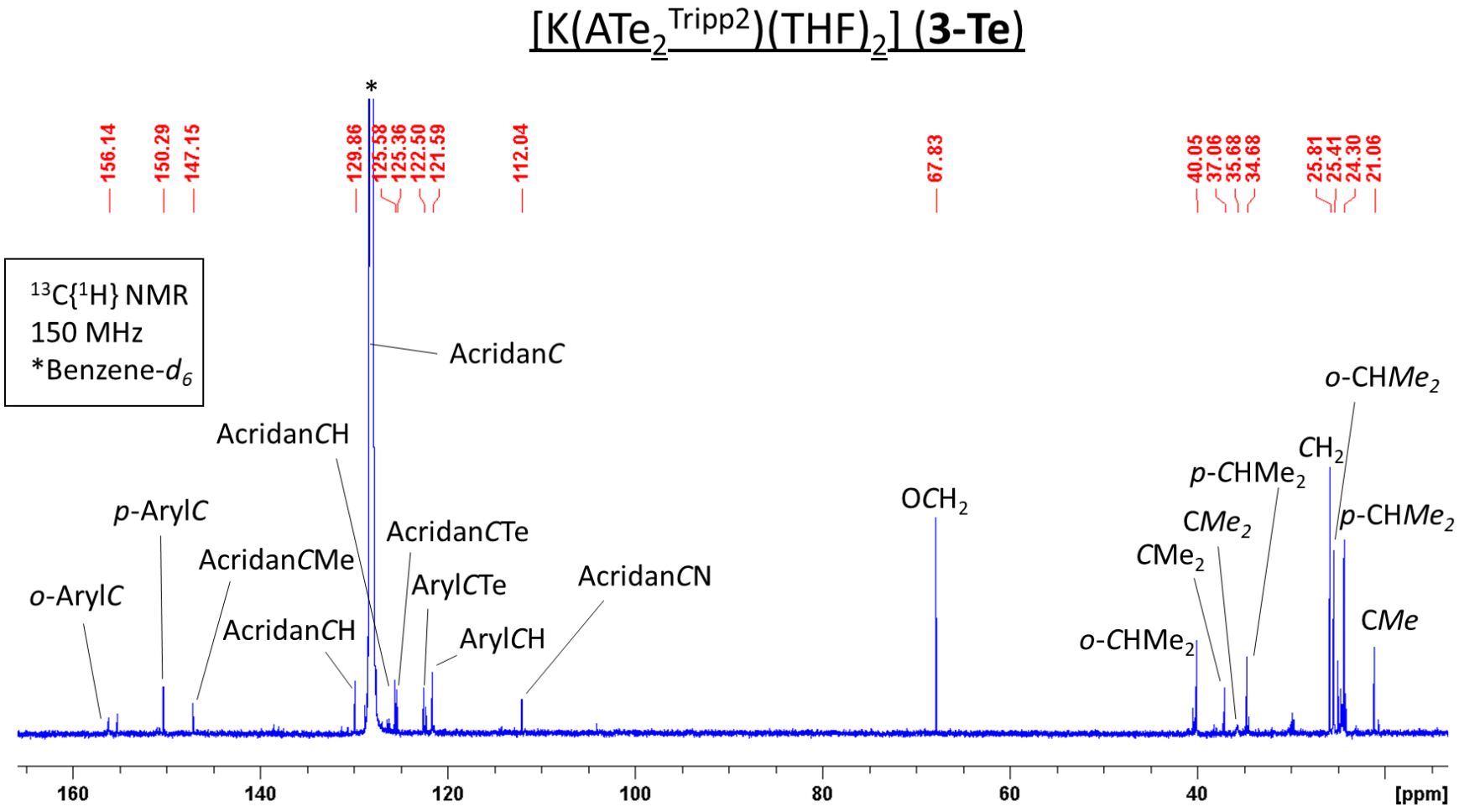

Figure S3. $^{13}C\{^{1}H\}$ NMR spectrum of $[K(ATe_2^{Tripp2})(THF)_2]$ (**3-Te**) in C_6D_6 (298 K).

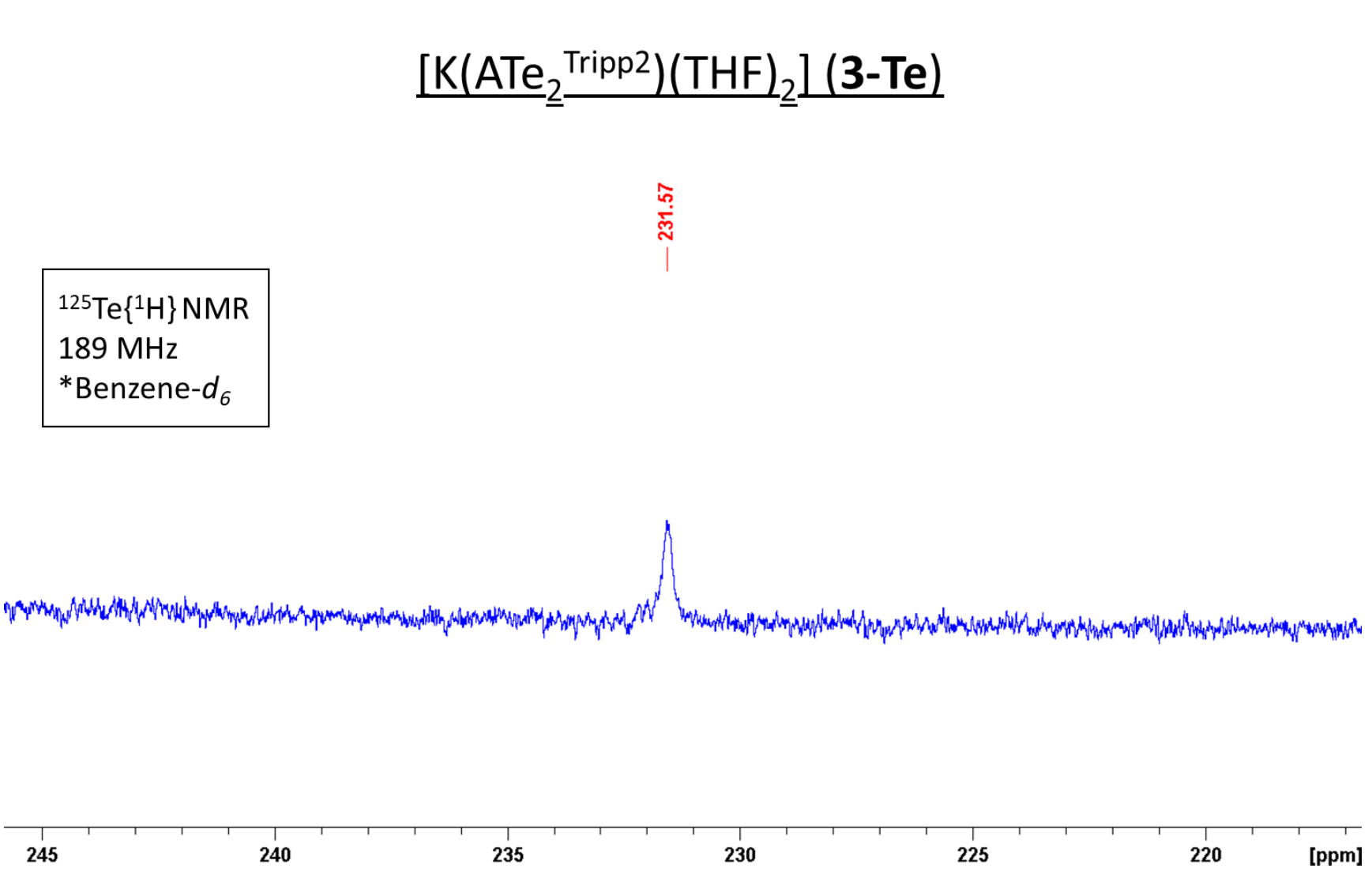

Figure S4. $^{125}Te\{^{1}H\}$ NMR spectrum of $[K(ATe_2^{Tripp2})(THF)_2]$ (**3-Te**) in C_6D_6 (298 K).

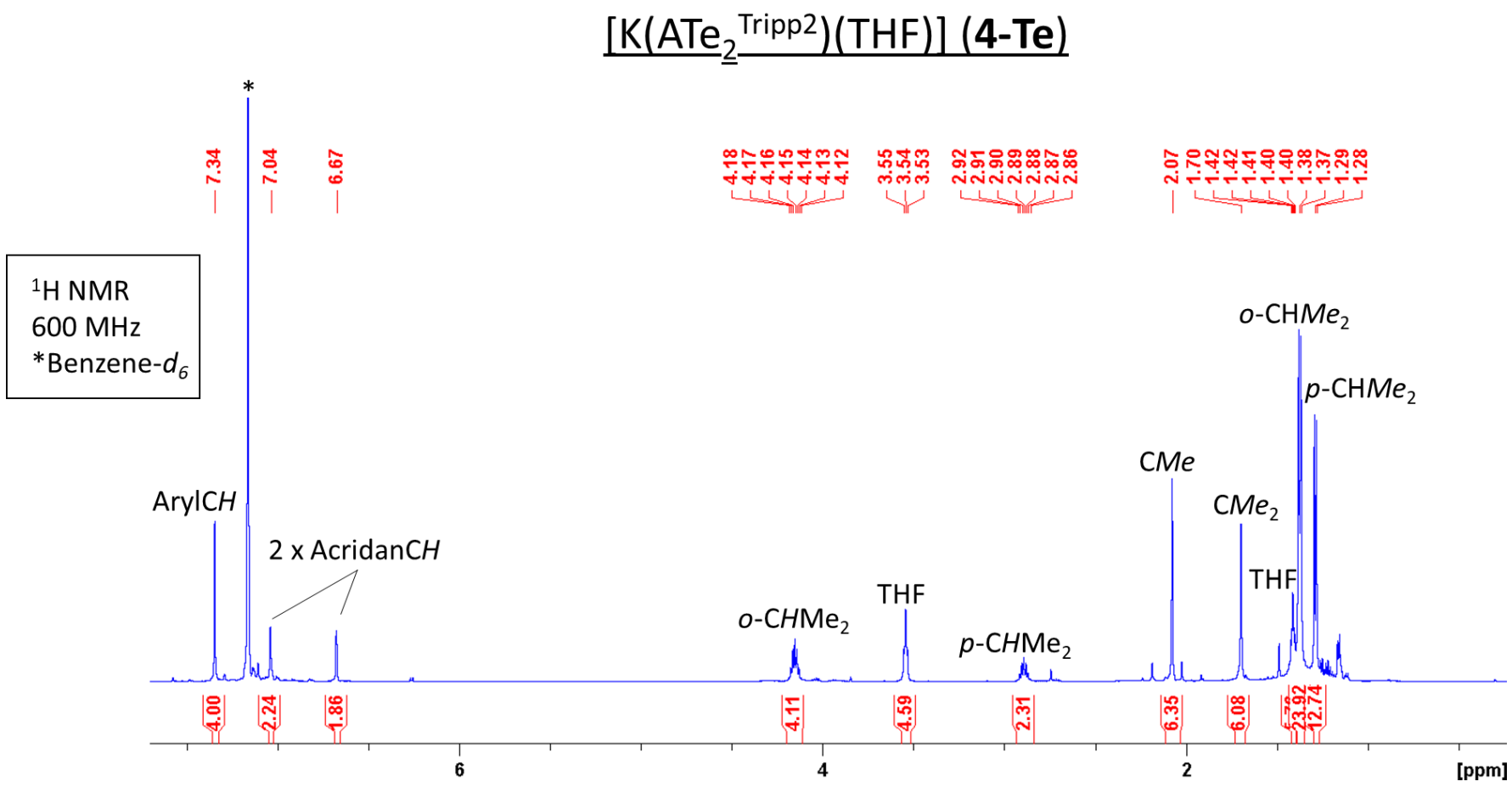

Figure S5. ^{1}H NMR spectrum of [K(ATe$_2^{Tripp2}$)(THF)] (**4-Te**) in C_6D_6 (298 K).

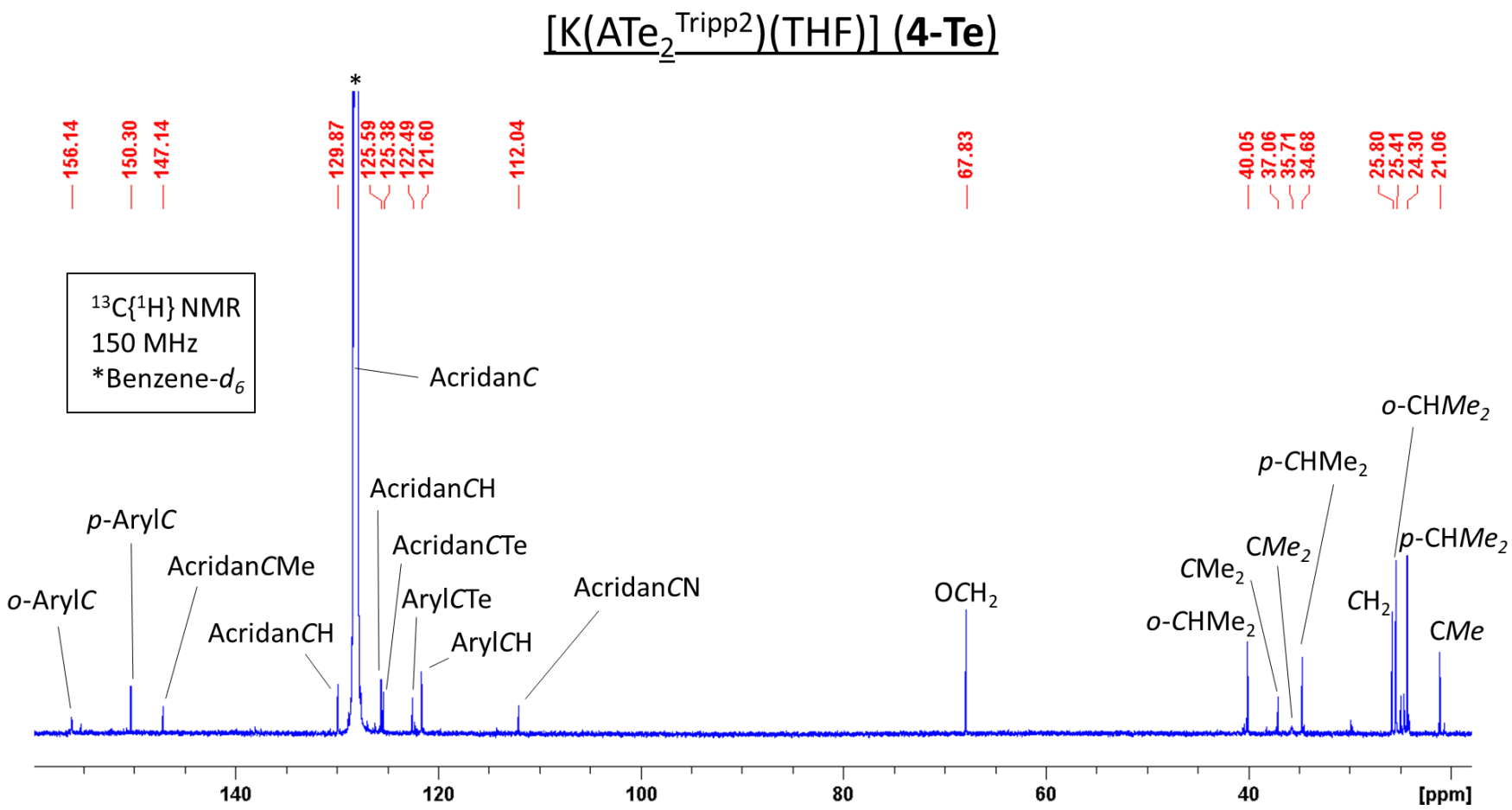

Figure S6. $^{13}C\{^{1}H\}$ NMR spectrum of [K(ATe_2^{Tripp2})(THF)] (**4-Te**) in C_6D_6 (298 K).

[K(ATe$_2^{Tripp2}$)(THF)] (**4-Te**)

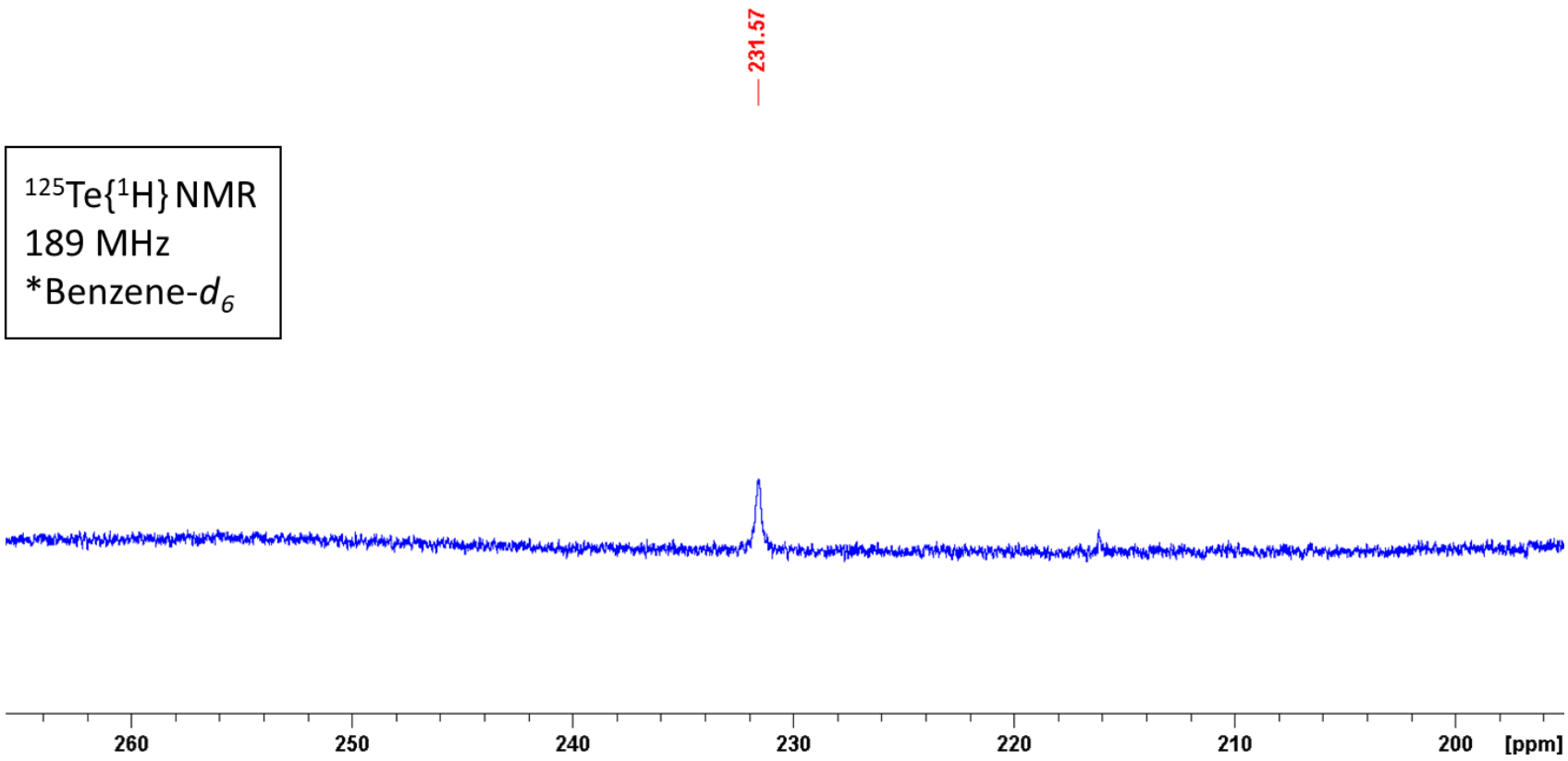

Figure S7. ^{125}Te{^{1}H} NMR spectrum of [K(ATe$_2^{Tripp2}$)(THF)] (**4-Te**) in C_6D_6 (298 K).

[K(ATe$_2^{Tripp2}$)]$_x$ (**5-Te**)

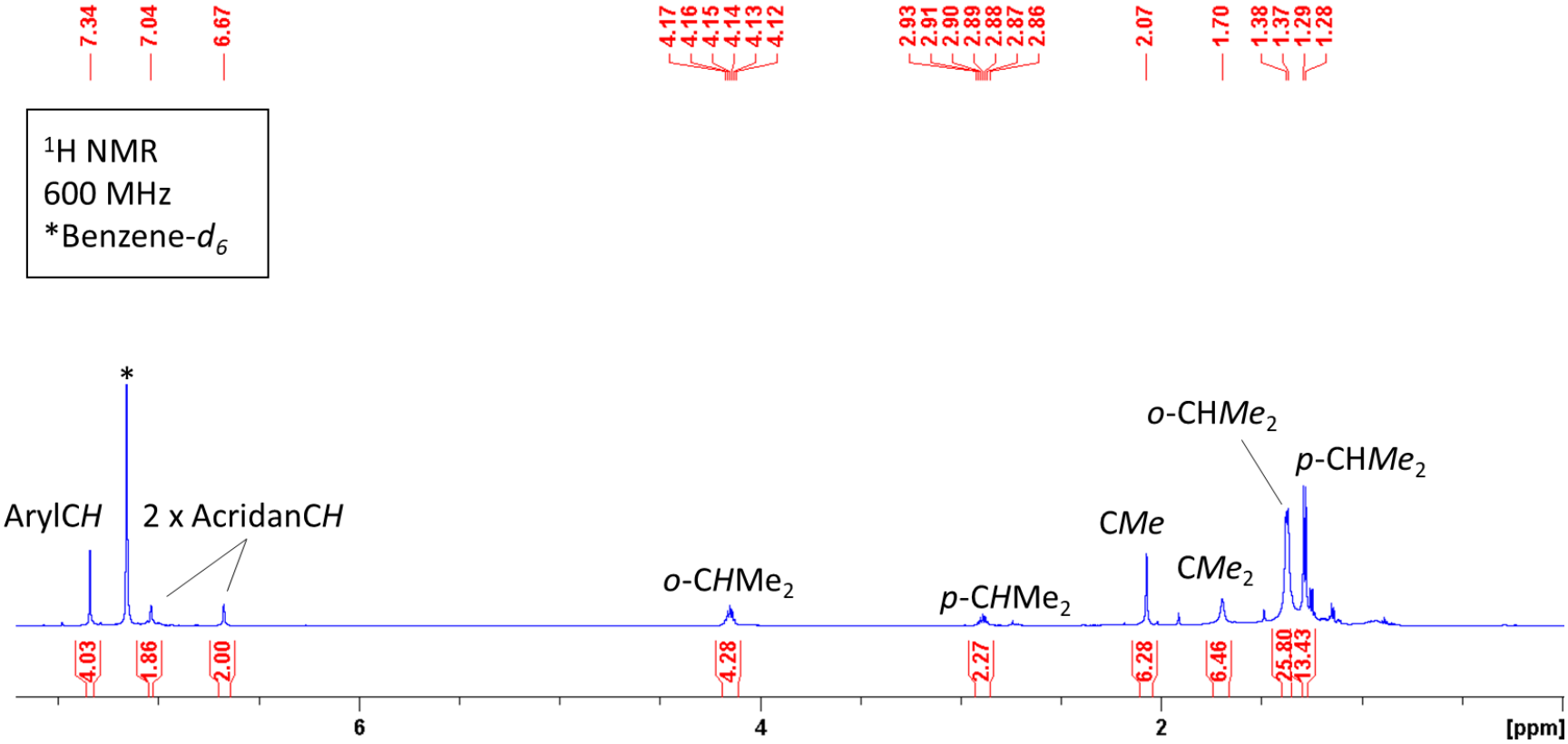

Figure S8. ^{1}H NMR spectrum of [K(ATe$_2^{Tripp2}$)]$_x$ (**5-Te**) in C_6D_6 (298 K).

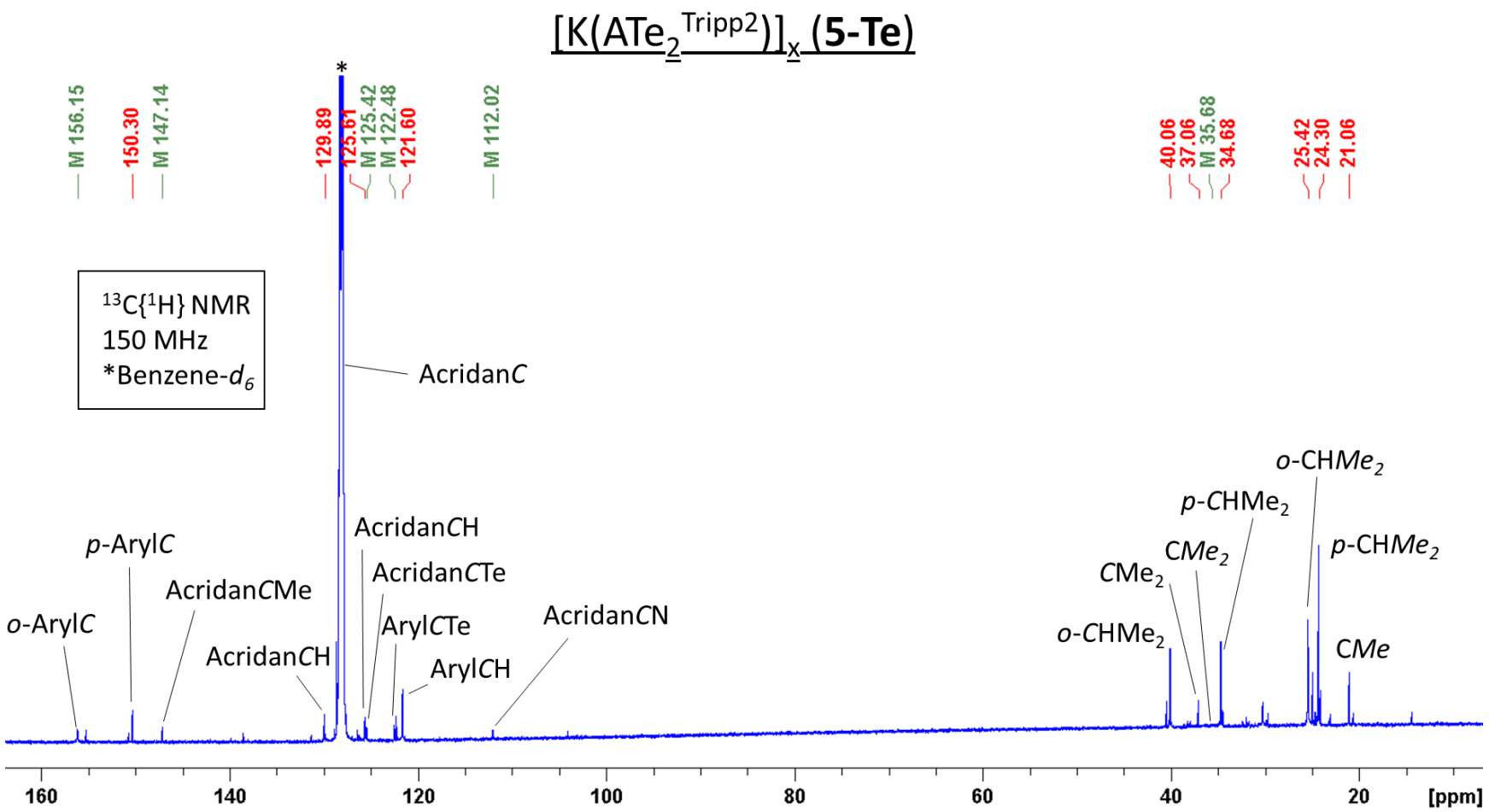

Figure S9. $^{13}C\{^{1}H\}$ NMR spectrum of $[K(ATe_2^{Tripp2})]_x$ (**5-Te**) in C_6D_6 (298 K).

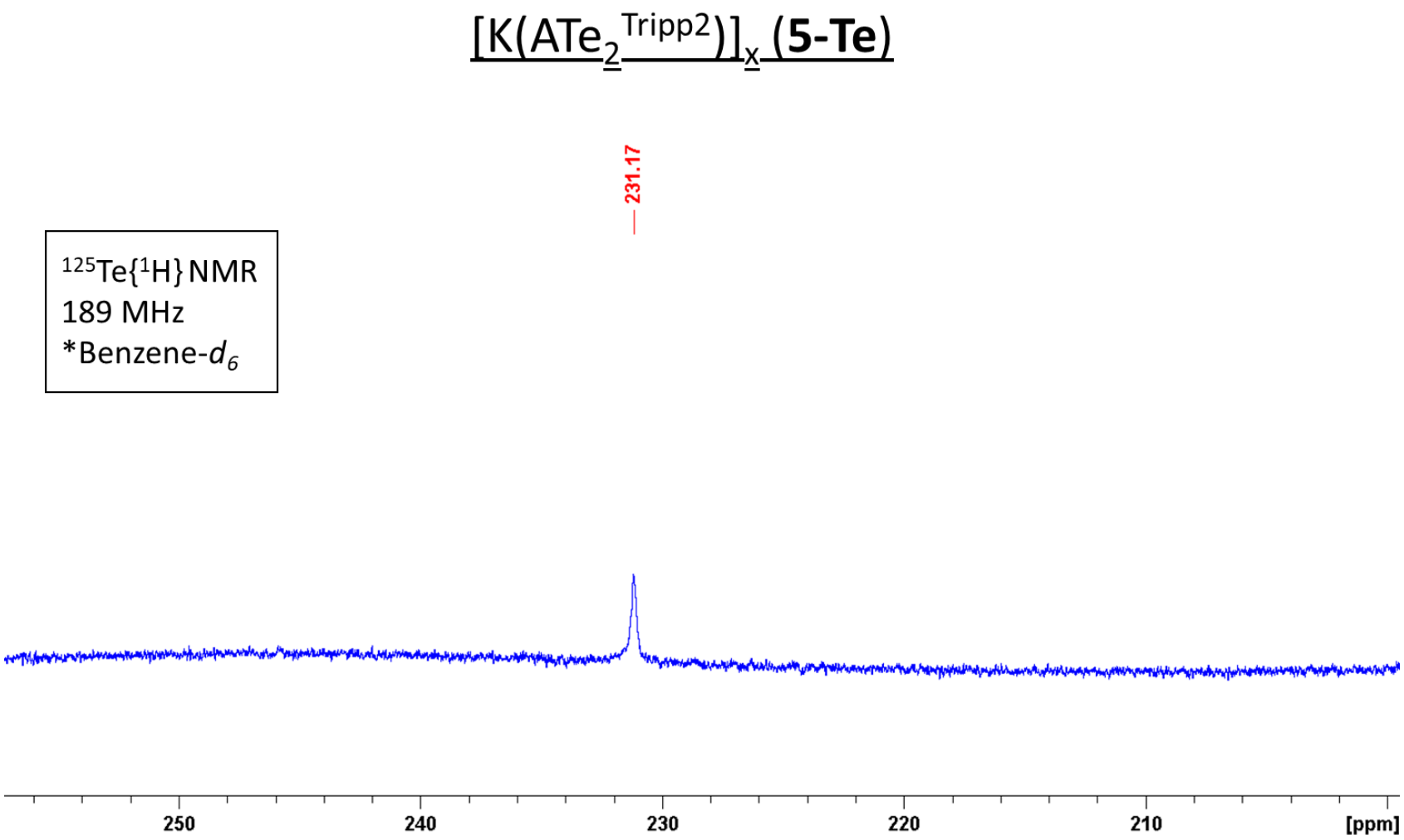

Figure S10. $^{125}Te\{^{1}H\}$ NMR spectrum of $[K(ATe_2^{Tripp2})]_x$ (**5-Te**) in C_6D_6 (298 K).

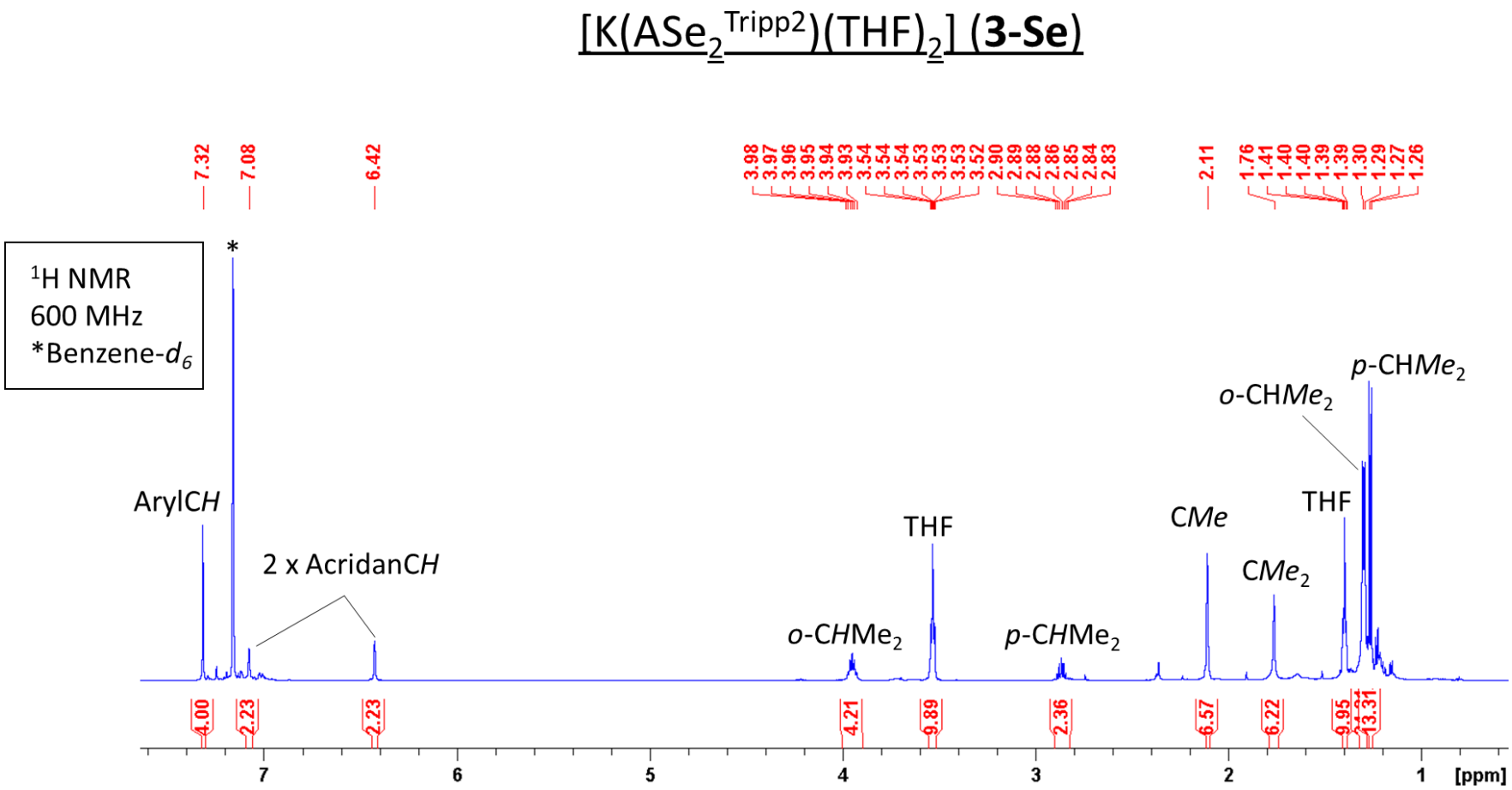

Figure S11. ^{1}H NMR spectrum of [K(ASe$_2$^{Tripp2})(THF)$_2$] (**3-Se**) in C_6D_6 (298 K).

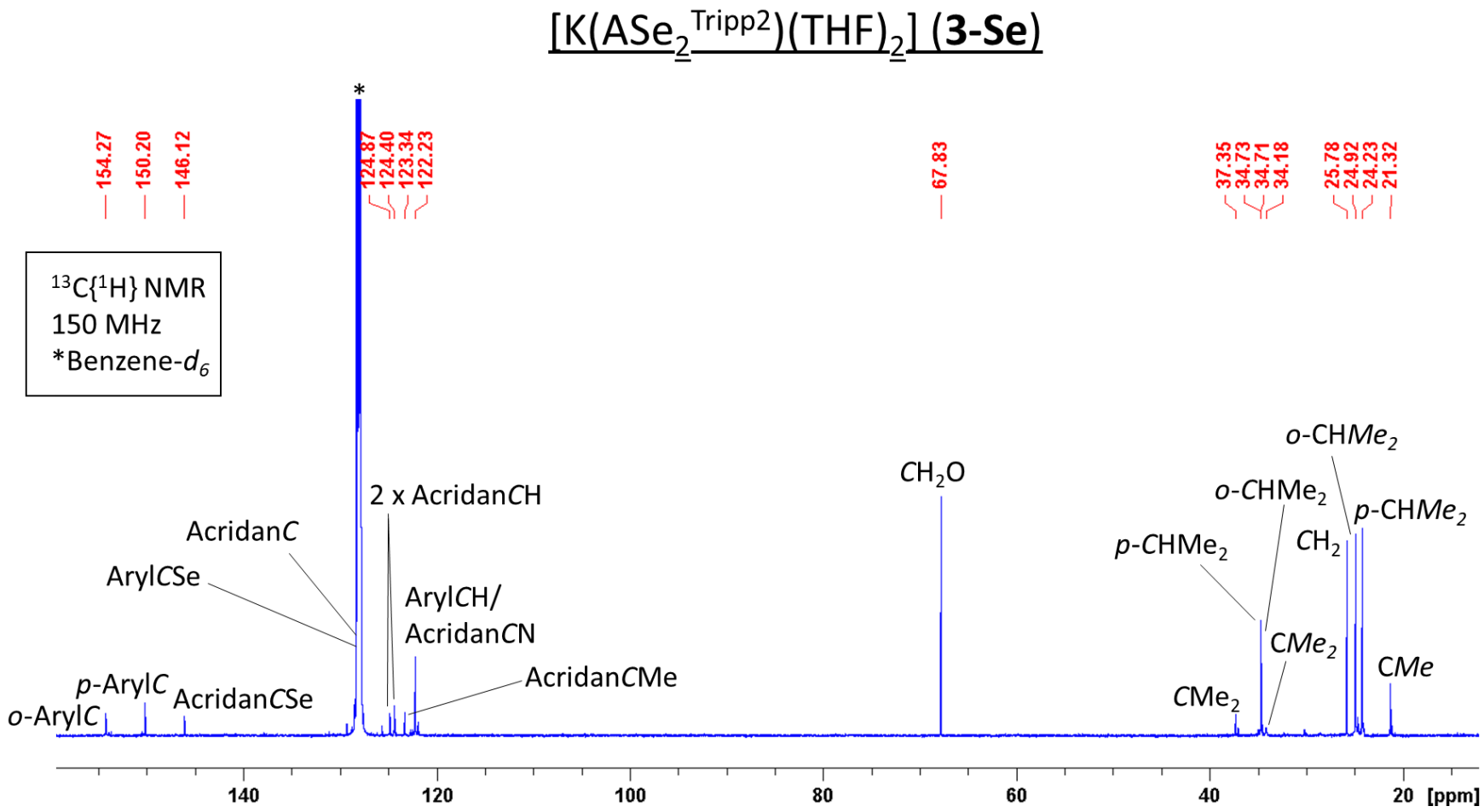

Figure S12. $^{13}C\{^{1}H\}$ NMR spectrum of [K(ASe_2^{Tripp2})$(THF)_2$] (**3-Se**) in C_6D_6 (298 K).

[K(ASe$_2$^{Tripp2})(THF)$_2$] (**3-Se**)

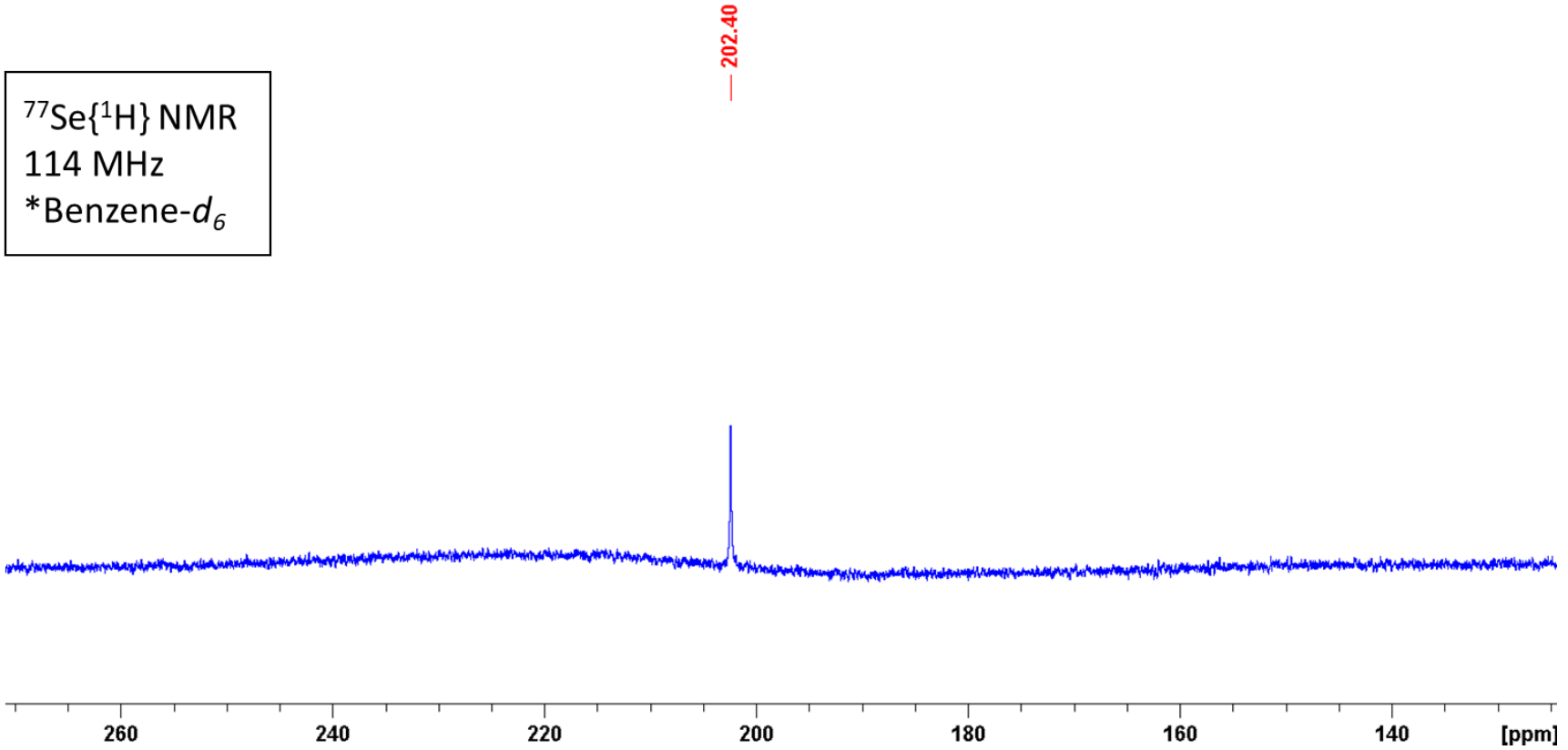

Figure S13. ^{77}Se{^{1}H} NMR spectrum of [K(ASe$_2$^{Tripp2})(THF)$_2$] (**3-Se**) in C_6D_6 (298 K).

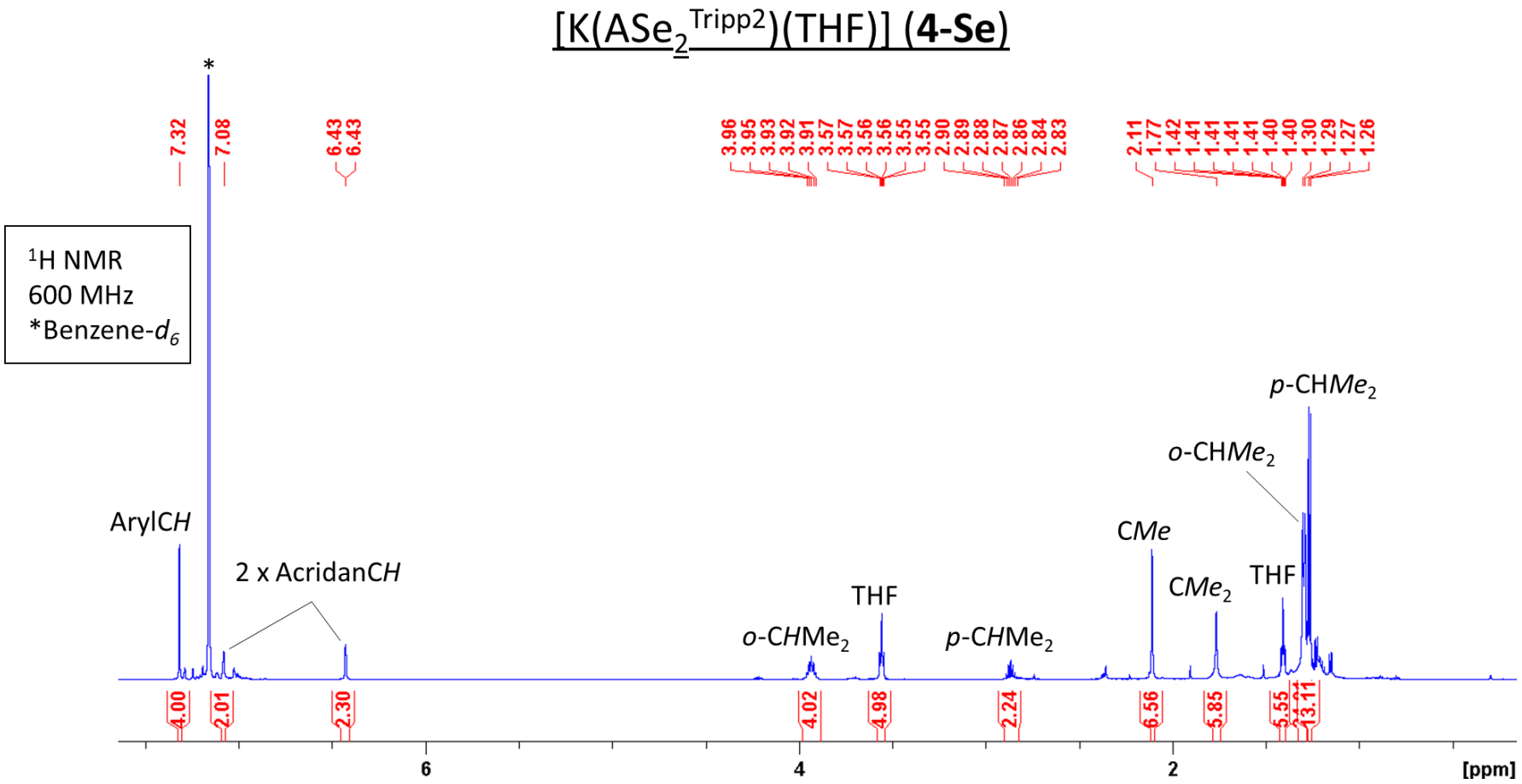

Figure S14. ^{1}H NMR spectrum of [K(ASe$_2$^{Tripp2})(THF)] (**4-Se**) in C_6D_6 (298 K).

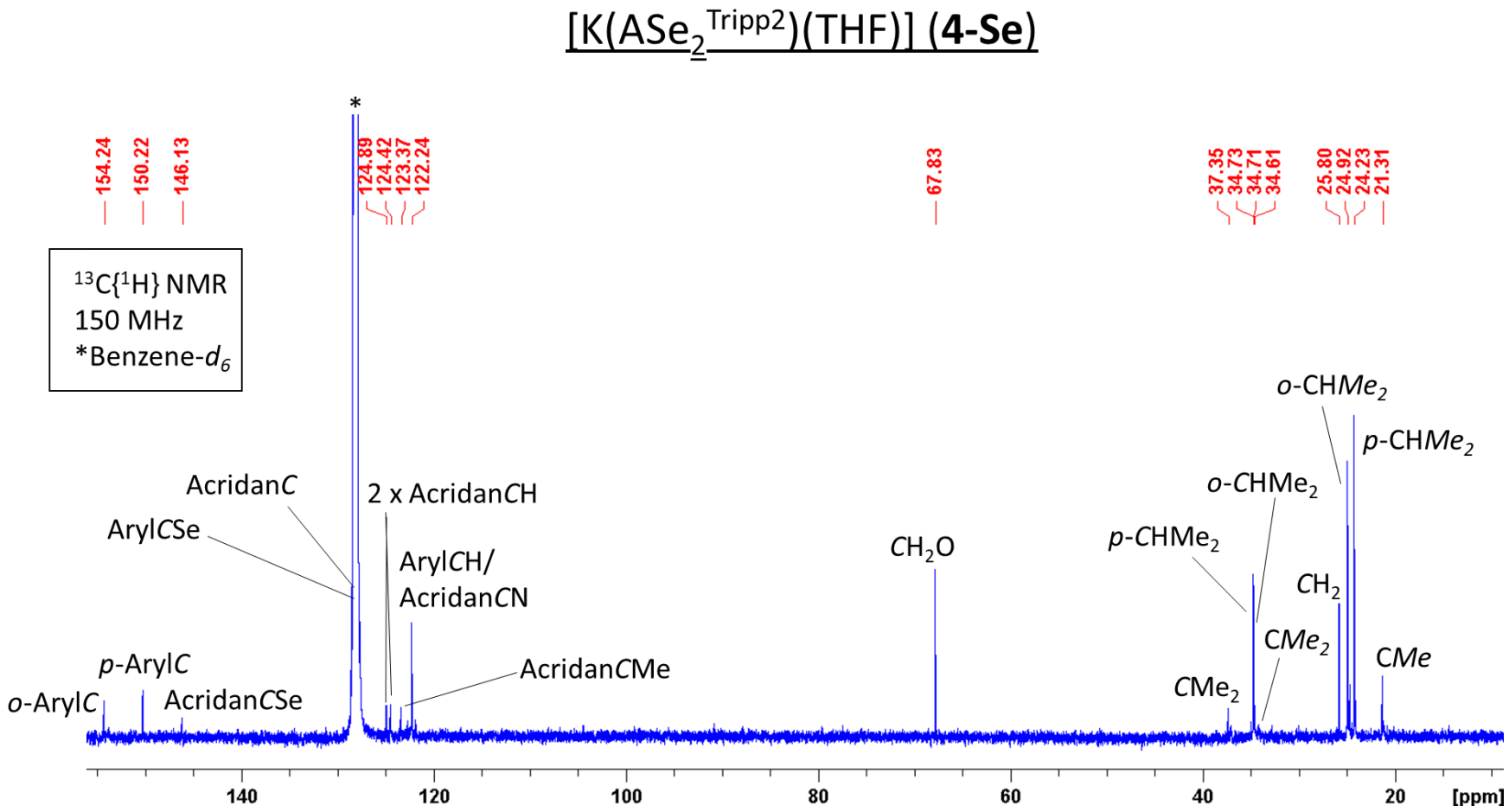

Figure S15. $^{13}C\{^{1}H\}$ NMR spectrum of [K(ASe_2^{Tripp2})(THF)] (**4-Se**) in C_6D_6 (298 K).

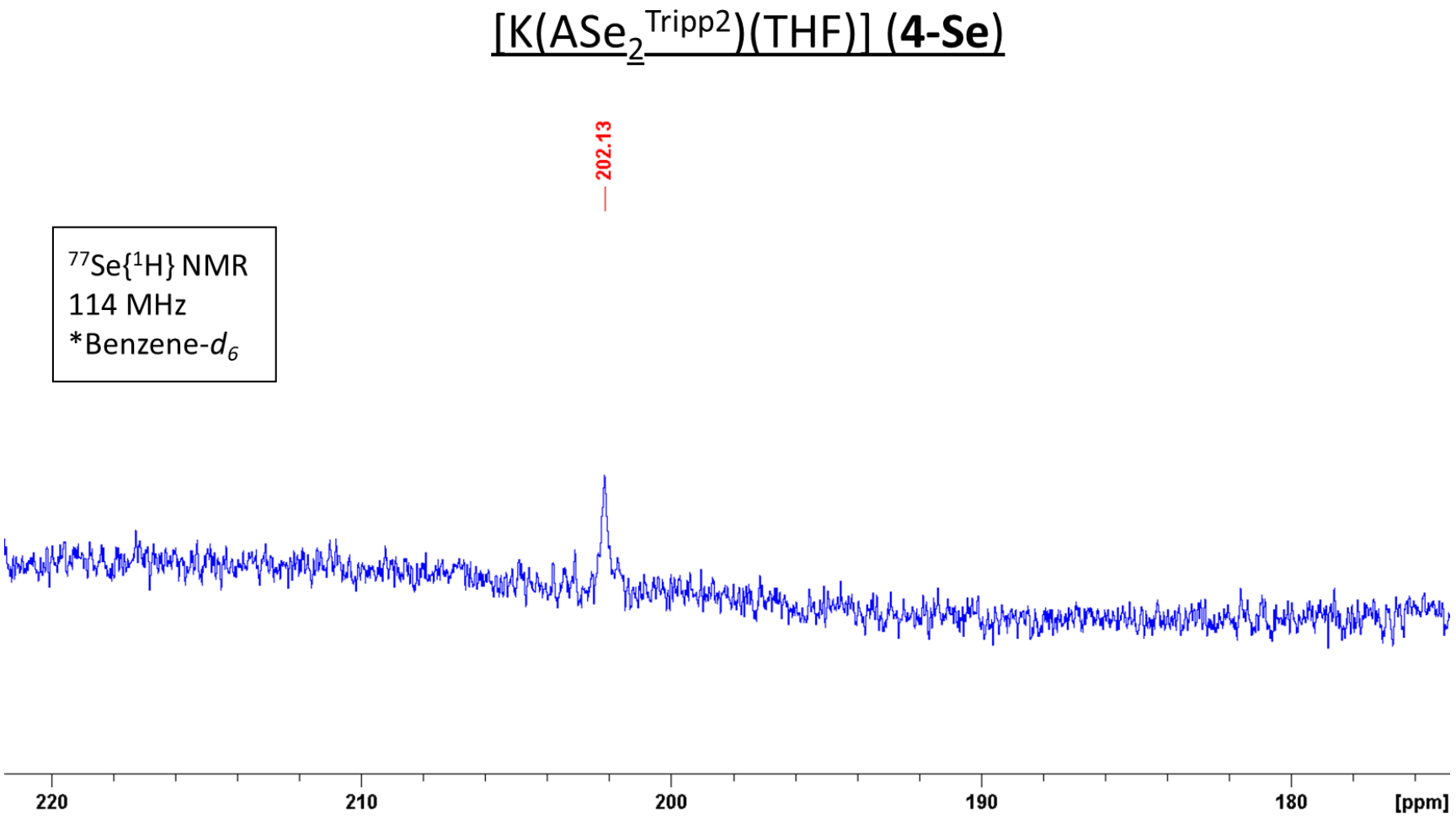

Figure S16. $^{77}Se\{^{1}H\}$ NMR spectrum of [K(ASe_2^{Tripp2})(THF)] (**4-Se**) in C_6D_6 (298 K).

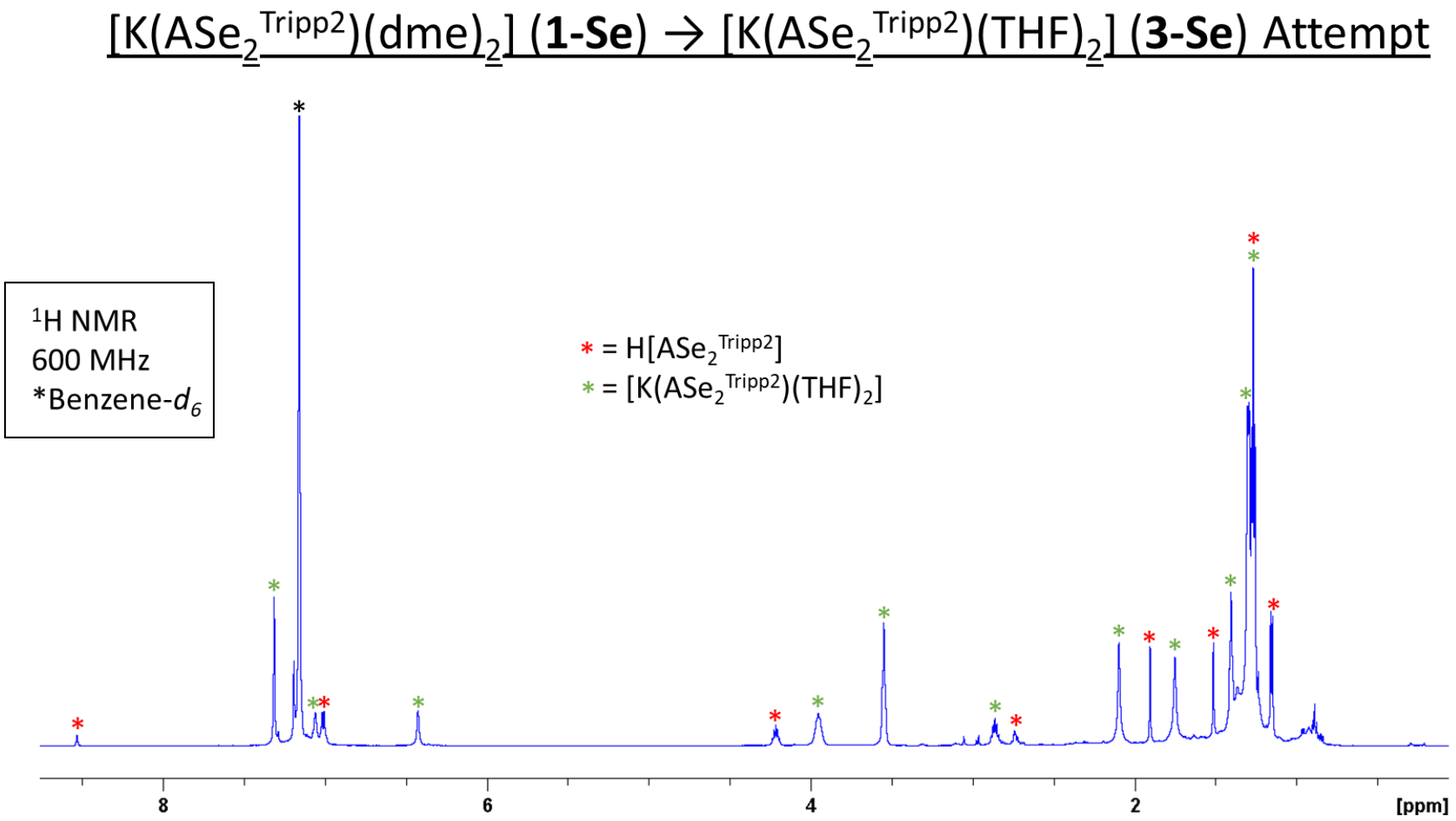

Figure S17. ^{1}H NMR spectrum of [K(ASe$_2^{Tripp2}$)(THF)$_2$] (**1-Se**) and pro-ligand in C_6D_6 (298 K) generated from repeated (three) dissolutions of [K(ASe$_2^{Tripp2}$)(dme)$_2$] (**1-Se**) in THF and evaporation of the solvent.

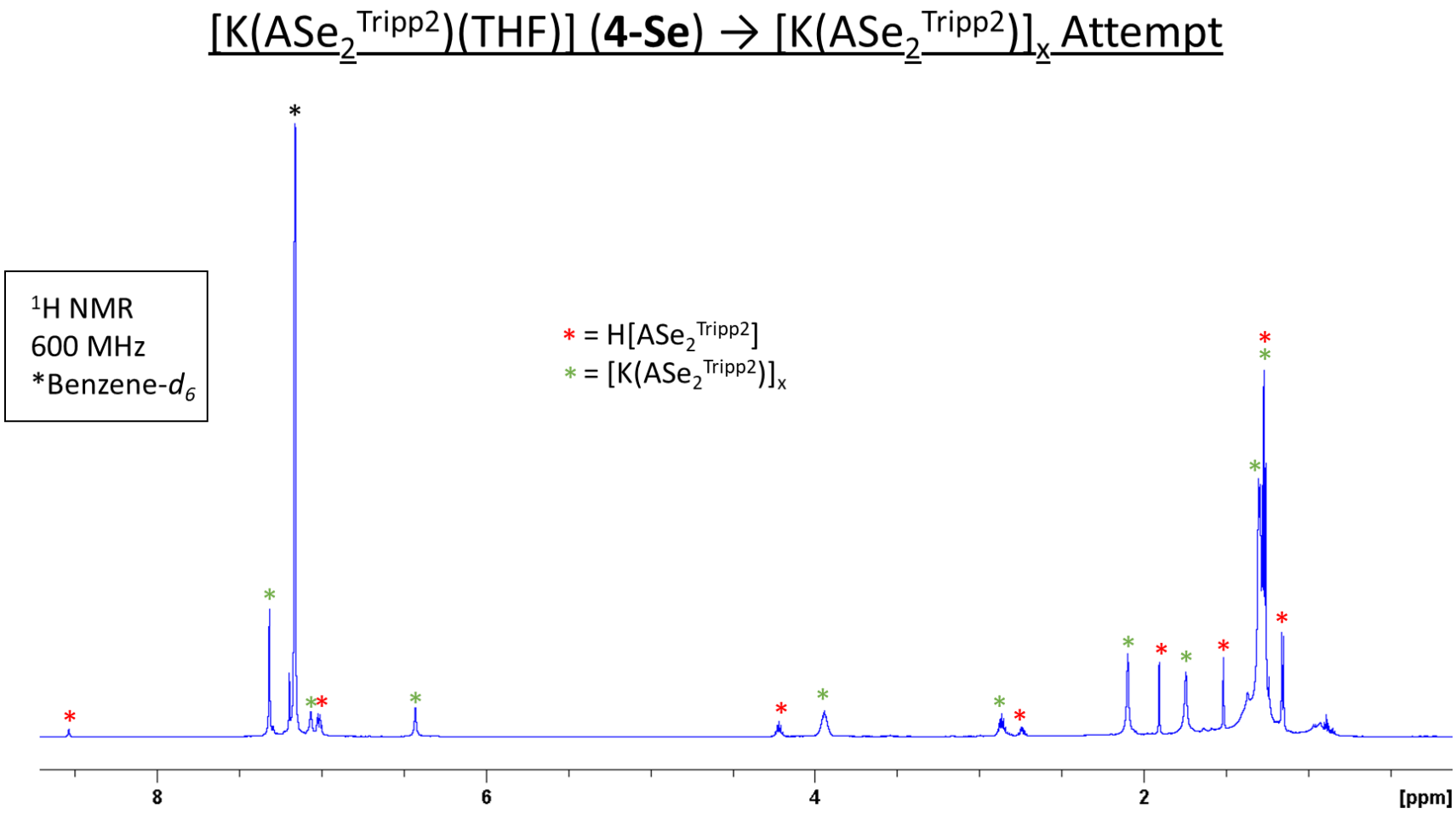

Figure S18. ^{1}H NMR spectrum of $[K(ASe_2^{Tripp2})]_x$ and pro-ligand in C_6D_6 (298 K) generated from repeated (two) dissolutions of $[K(ASe_2^{Tripp2})(THF)]$ (**4-Se**) in benzene and evaporation of the solvent.

Computational Data

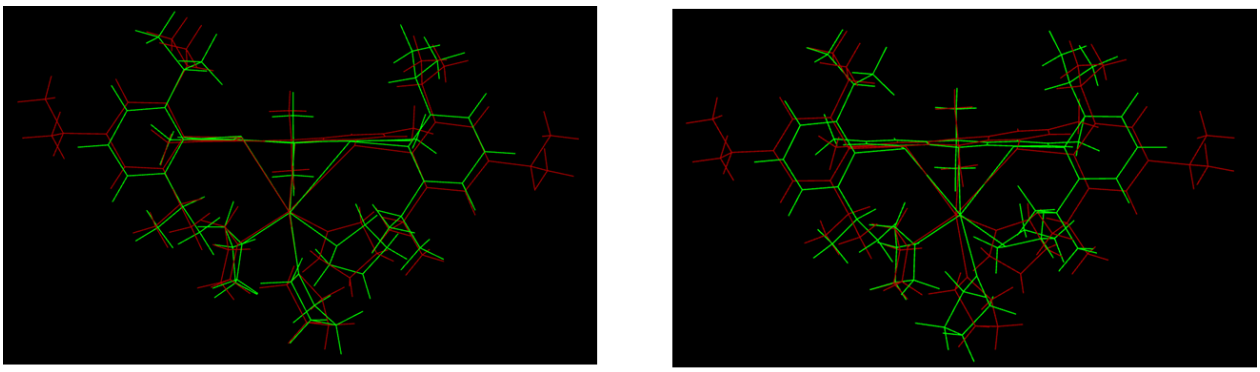

Figure S19. Overlay of the X-ray crystal structures (red) [K(ATe$_2^{Tripp2}$)(THF)$_3$] (**2-Te**) and [K(ASe$_2^{Tripp2}$)(THF)$_3$] (**2-Se**) and their respective DFT models (green) [K(ATe$_2^{Dipp2}$)(THF)$_3$] **2-Te*** and [K(ASe$_2^{Dipp2}$)(THF)$_3$] **2-Se***.

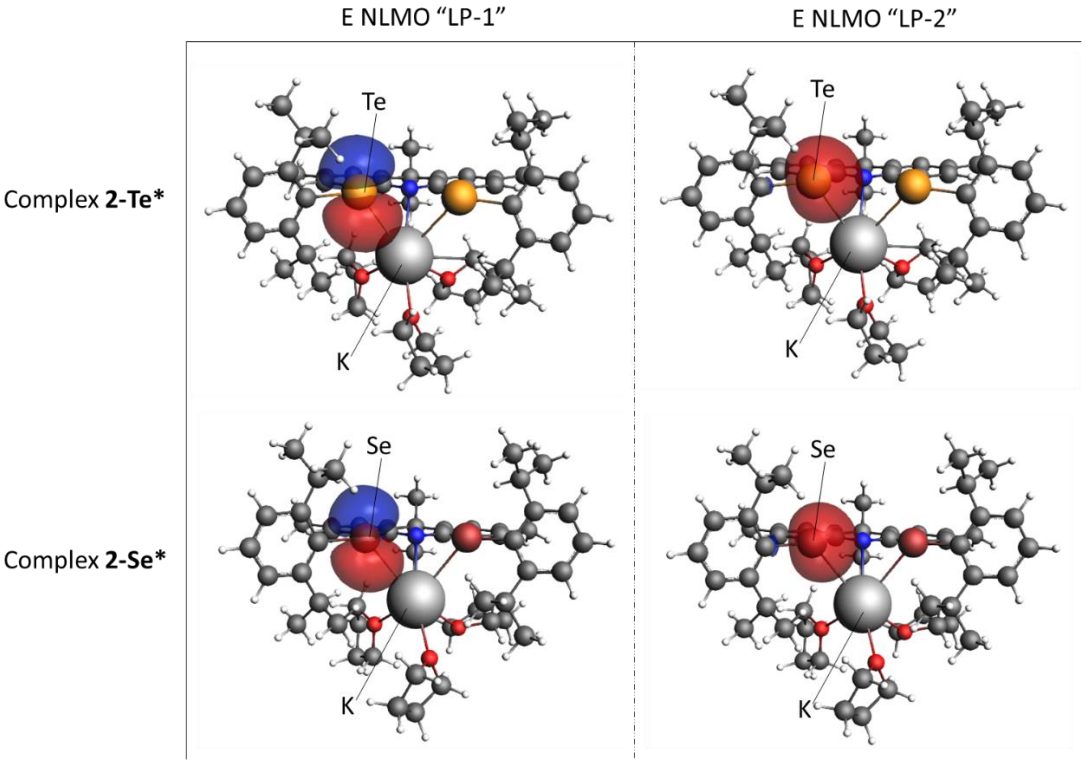

Figure S20. Representative E (Se or Te) NLMOs in calculated complexes **2-Te*** and **2-Se***. Isosurfaces are set to 0.03.

Table S1. Selected bond distances for the calculated structures **2-Te*** and **2-Se***. Values in un-bolded black font correspond to the calculated distances. X-ray structure metrics are reported in bold with curly brackets.

DFT Complex	K–E distances (Å) (E = Se, Te)	K–N distances (Å)	K–O distances (Å)
$[K(ATe_2^{Dipp2})(THF)_3]$ (**2-Te***)	3.582, 3.640 **{3.496(2), 3.639(2)}**	2.840 **{2.824(4)}**	2.714, 2.736, 2.755 **{2.584(5), 2.691(5), 2.693(5)}**
$[K(ASe_2^{Dipp2})(THF)_3]$ (**2-Se***)	3.426, 3.429 **{3.397(4), 3.472(4)}**	2.818 **{2.82(1)}**	2.747, 2.783, 2.805 **{2.67(1), 2.68(1), 2.79(1)}**

Table S2. Selected QTAIM, NBO and Mayer bond order data for the K–E interactions (E = Se, Te) in **2-Te*** and **2-Se***. The E lone pair NLMOs are denoted as "LP-1" and "LP-2" (see Figure S20). NLMOs have been normalized to include only metal and chalcogen contributions.

DFT Complex	K–E Mayer Bond Orders	δ K–E	H_b K–E (au)	% K in E NLMO, "LP-1" (normalized)	% K in E NLMO, "LP-2" (normalized)
$[K(ATe_2^{Dipp2})(THF)_3]$ (**2-Te***)	0.08, 0.10	0.0678, 0.0736	0.00010, 0.0010	0.51%, 0.53%	0.73%, 0.71%
$[K(ASe_2^{Dipp2})(THF)_3]$ (**2-Se***)	0.07, 0.08	0.0673 0.0671	0.0013, 0.0013	0.24%, 0.19%	0.69%, 0.68%

Table S3. Potassium and chalcogen (Se or Te) atomic orbital compositions in the E lone pair NLMO's (denoted as "LP-1" and "LP-2"; see Figure S20) for **2-Te*** and **2-Se***.

DFT Complex	E atomic orbital composition in "LP-1" (%)	E atomic orbital composition in "LP-2" (%)	M atomic orbital composition in "LP-1" (%)	M atomic orbital composition in "LP-2" (%)
$[K(ATe_2^{Dipp2})(THF)_3]$ (**2-Te***)	*s* (0.37-0.67), *p* (99.28-99.58), *d* (0.04), *f* (0.01)	*s* (78.21-78.38), *p* (21.60-21.77), *d* (0.01), *f* (0.00)	*s* (79.80-83.18), *p* (2.06-2.07), *d* (14.64-18.03), *f* (0.11)	*s* (99.21-99.24), *p* (0.14-0.18), *d* (0.54-0.60), *f* (0.05)
$[K(ASe_2^{Dipp2})(THF)_3]$ (**2-Se***)	*s* (0.07-0.13), *p* (99.81-99.86), *d* (0.05-0.06), *f* (0.01)	*s* (74.54-74.56), *p* (25.41-25.43), *d* (0.02), *f* (0.00)	*s* (59.00-66.19), *p* (2.71-3.54), *d* (30.79-37.12), *f* (0.30-0.34)	*s* (98.13-98.55), *p* (0.26-0.32), *d* (1.13-1.48), *f* (0.07-0.08)

Table S4. Selected QTAIM, NBO and Mayer bond order data for the K–X interactions (X = N or O) in **2-Te***, **2-Te*$_{Constr}$** and **2-Se***. The K–N and K–O NLMOs have been normalized to include only metal and donor atom contributions.

DFT Complex	K–N Mayer Bond Orders	K–O Mayer Bond Orders	δ K–N	δ K–O	H_b K–N (au)	H_b K–O (au)	% K in K–N NLMO (normalized)	% K in K–O NLMO (normalized)
$[K(ATe_2^{Dipp2})(THF)_3]$ (**2-Te***)	<0.05	0.05, 0.05, <0.05	0.0973	0.0923, 0.0944, 0.0954	0.0021	0.0031, 0.0033, 0.0035	0.13%	0.23%, 0.23%, 0.24%
$[K(ASe_2^{Dipp2})(THF)_3]$ (**2-Se***)	<0.05	0.05, <0.05, <0.05	0.102	0.0908, 0.0860, 0.0816	0.0021	0.0033, 0.0031, 0.0030	0.19%	0.41%, 0.22%, 0.25%,

SHAPE Parameters

Table S5. Continuous shape measures (CSMs) of the 6-coordinate potassium coordination polyhedra in the X-ray crystal structures of **2-Te** and **2-Se**. The values in red indicate the closest polyhedron according to the CSM's, while the values in blue indicate the second closest polyhedron according to the CSMs.

Polyhedron	Symmetry	CSM of 6-coordinate potassium coordination polyhedra	
		2-Te	**2-Se**
hexagon (HP-6)	D_{6h}	25.288	23.176
pentagonal pyramid (PPY-6)	C_{5v}	23.401	20.586
octahedron (OC-6)	O_h	**7.268**	**7.889**
trigonal prism (TPR-6)	D_{3h}	13.249	12.028
Johnson pentagonal pyramid (JPPY-6)	C_{5v}	25.701	22.818

Table S6. Continuous shape measures (CSMs) of the 5-coordinate potassium coordination polyhedra in the X-ray crystal structures of **5-Te** and **3-Se**. The values in red indicate the closest polyhedron according to the CSM's, while the values in blue indicate the second closest polyhedron according to the CSMs.

Polyhedron	Symmetry	CSM of 5-coordinate potassium coordination polyhedral**	
		5-Te	**3-Se**
pentagon (PP-5)	D_{5h}	32.143	29.840
vacant octahedron (vOC-5)	C_{4v}	15.913	9.469
trigonal bipyramid (TBPY-5)	D_{3h}	**15.736***	10.892
spherical square pyramid (SPY-5)	C_{4v}	16.818	**9.218**
Johnson trigonal bipyramid (JTBPY-5)	D_{3h}	17.581	14.277

* The coordination geometry in **5-Te** is not a strong match to any regular polyhedron.

** The coordination geometries of **5-Te** and **3-Se** match with multiple different polyhedra to a similar extent.

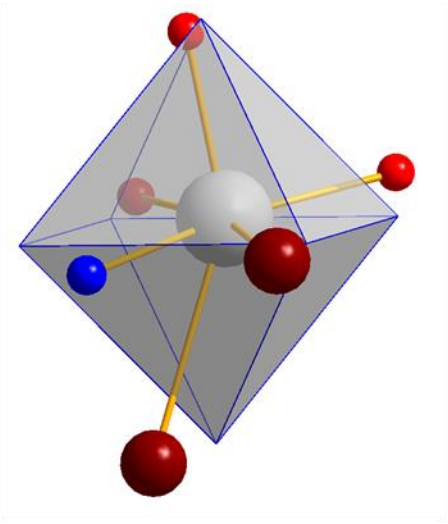

$[K(ATe_2^{Tripp2})(THF)_3]$ (**2-Te**)

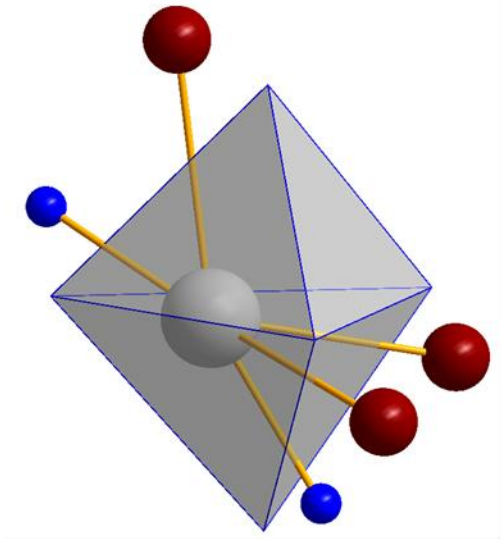

$[K(ATe_2^{Tripp2})]_x$ (**5-Te**)

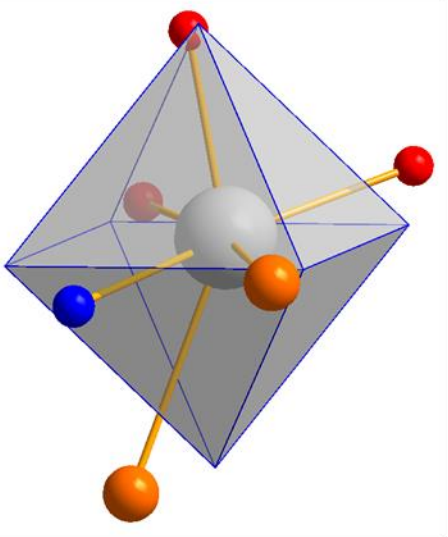

$[K(ASe_2^{Tripp2})(THF)_3]$ (**2-Se**)

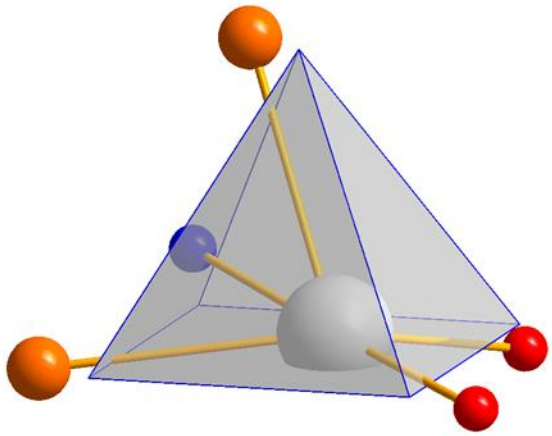

$[K(ASe_2^{Tripp2})(THF)_2]$ (**3-Se**)

Figure S21. Closest fits, according to the SHAPE program, for the coordination geometry around potassium in the X-ray structures of $[K(ATe_2^{Tripp2})(THF)_3]$ (**2-Te**; top left), $[K(ATe_2^{Tripp2})(THF)_3]$ (**5-Te**; top right), $[K(ASe_2^{Tripp2})(THF)_3]$ (**2-Se**; bottom left) and $[K(ASe_2^{Tripp2})(THF)_2]$ (**3-Se**; bottom right). Idealized polyhedra which most closely match the geometry of each structure have been superimposed (**2-Te** and **2-Se**; octahedron, **5-Te**; trigonal bipyramid, **3-Se**; spherical square pyramid). Atoms in the coordination environment are represented by spheres; potassium (grey), nitrogen (blue), oxygen (red), selenium (orange), tellurium (burgundy).

References:

1 P. J. Bailey, R. A. Coxall, C. M. Dick, S. Fabre, L. C. Henderson, C. Herber, S. T. Liddle, D. Loroño-González, A. Parkin and S. Parsons, *Chem. − Eur. J.*, 2003, **9**, 4820.

2 N. A. G. Gray, I. Vargas-Baca and D. J. H. Emslie, *Inorg. Chem.*, 2023, **62**, 16974.

3 R. K. Harris, E. D. Becker, S. M. Cabral de Menezes, R. Goodfellow and P. Granger, 2001, **73**, 1795.

4 G. M. Sheldrick, *Acta Crystallogr., Sect. A: Found. Adv.*, **2015**, *71*, 3−8.

5 G. M. Sheldrick, *Acta Crystallogr., Sect. C: Struct. Chem.*, **2015**, *71*, 3−8.

6 O. V. Dolomanov, L. J. Bourhis, R. J. Gildea, J. K. A. Howard, H. Puschmann, *J. Appl. Crystallogr.*, **2009**, *42*, 339−341.

7 (*a*) ADF 2020, SCM, Theoretical Chemistry, Vrije Universiteit, Amsterdam, The Netherlands, http://www.scm.com; (*b*) C. F. Guerra, J. G. Snijders, G. te Velde and E. J. Baerends, *Theor. Chem. Acc.*, **1998**, *99* (6), 391-403; (*c*) G. te Velde, F. M. Bickelhaupt, E. J. Baerends, C. Fonseca Guerra, S. J. A. Van Gisbergen, J. G. Snijders and T. Ziegler, *J. Comput. Chem.*, **2001**, *22* (9), 931-967

8 J. P. Perdew, K. Burke and M. Ernzerhof, *Phys. Rev. Lett.*, 1996, **77**, 3865.

9 E. v. Lenthe, E. J. Baerends and J. G. Snijders, *J. Chem. Phys.*, 1993, **99**, 4597.

10 E. van Lenthe, E. J. Baerends and J. G. Snijders, *J. Chem. Phys.*, 1994, **101**, 9783.

11 E. van Lenthe, A. Ehlers and E.-J. Baerends, *J. Chem. Phys.*, 1999, **110**, 8943.

12 E. van Lenthe, J. G. Snijders and E. J. Baerends, *J. Chem. Phys.*, 1996, **105**, 6505.

13 E. van Lenthe, R. van Leeuwen, E. J. Baerends and J. G. Snijders, *Int. J. Quantum Chem.*, 1996, **57**, 281.

14 S. Grimme, J. Antony, S. Ehrlich and H. Krieg, *J. Chem. Phys.*, 2010, **132**, 154104.

15 S. Grimme, S. Ehrlich and L. Goerigk, *J. Comput. Chem.*, 2011, **32**, 1456.

16 A. D. Becke, *J. Chem. Phys.*, 1988, **88**, 2547.

17 M. Franchini, P. H. T. Philipsen and L. Visscher, *J. Comput. Chem.*, 2013, **34**, 1819.

18 A. Bérces, R. M. Dickson, L. Fan, H. Jacobsen, D. Swerhone and T. Ziegler, *Comput. Phys. Commun.*, 1997, **100**, 247.

19 H. Jacobsen, A. Bérces, D. P. Swerhone and T. Ziegler, *Comput. Phys. Commun.*, 1997, **100**, 263.

20 S. K. Wolff, *Int. J. Quantum Chem.*, 2005, **104**, 645.

21 R. F. W. Bader, *Atoms in Molecules: A Quantum Theory*, Clarendon Press, Oxford, 1990.

22 J. I. Rodríguez, R. F. W. Bader, P. W. Ayers, C. Michel, A. W. Götz and C. Bo, *Chem. Phys. Lett.*, 2009, **472**, 149.

23 J. I. Rodríguez, A. M. Köster, P. W. Ayers, A. Santos-Valle, A. Vela and G. Merino, *J. Comput. Chem.*, 2009, **30**, 1082.

24 J. I. Rodríguez, *J. Comput. Chem.*, 2013, **34**, 681.

25 P. W. Ayers and S. Jenkins, *Comput. Theor. Chem.*, 2015, **1053**, 112.

26 V. Tognetti and L. Joubert, *Phys. Chem. Chem. Phys.*, 2014, **16**, 14539.

27 Y. A. Abramov, *Acta Crystallogr., Sect. A: Found. Crystallogr.*, **1997**, *A53*, 264-272.

28 X. Fradera, M. A. Austen and R. F. W. Bader, *J. Phys. Chem. A*, 1999, **103**, 304.

29 J. Poater, M. Solà, M. Duran and X. Fradera, *Theor. Chem. Acc.*, 2002, **107**, 362.

30 NBO 6.0: E. D. Glendening, J. K. Badenhoop, A. E. Reed, J. E. Carpenter, J. A. Bohmann, C. M. Morales, C. R. Landis, and F. Weinhold, Theoretical Chemistry Institute, University of Wisconsin, Madison, 2013.